Control performance of active-passive composite tuned mass damper

Smart Mater. Struct. **7** (1998) 637–653. Printed in the UK PII: S0964-1726(98)96192-4

Control performance of active–passive composite tuned mass damper

Isao Nishimura, Toshikazu Yamada, Mitsuo Sakamoto and Takuji Kobori

Kobori Research Complex, Kajima Corporation, KI Building, 6-5-30, Akasaka, Minato-ku, Tokyo 107, Japan

Received 28 January 1997, accepted for publication 1 July 1997

Abstract. This paper reviews an active control algorithm adopted for an active–passive composite tuned mass damper, which is a unique vibration control device equipped into an office building in Tokyo in 1993. The main purpose of this device is to subdue the response motion of tall buildings under random disturbances such as wind pressures and small earthquakes. The main topics in this paper are: (1) the principle of the acceleration feedback algorithm, (2) the expected control performance, (3) the multi-modal control algorithm, (4) the observed performance of the applications using the algorithm.

1. Background

The tuned mass damper (TMD) is a small oscillator which is attached to a primary system which is subjected to disturbance excitations. The natural frequency of the device is adjusted close to the primary system's natural frequency so that the vibration energy is transferred to the auxiliary system where it is dissipated away.

The tuned mass damper, otherwise known as a vibration absorber, is an invention by Frahm [5]. The original TMD, shown in figure 1, had no damping between its secondary mass and the primary system. Later, this vibration control device was studied by Ormondroyd and Den Hartog [4] and they discovered that some additional damping to the device, shown in figure 2, increases its control performance. But they did not clarify how to optimize its frequency response by adjusting the stiffness of the device. The frequency optimization based on the so-called 'lock-points' method was first studied by Erich Hahnkamm [6, 7]. He clarified that there is an optimum stiffness that reduces the response peak as much as possible. The result was later introduced into the first edition of *Mechanical Vibration* by Den Hartog. Later this phenomenon was further studied by Brock [1], who was motivated to study the device after reading *Mechanical Vibration*. He optimized the damping factor just like the stiffness by the 'lock-points' method. The final result was introduced into the revised edition of *Mechanical Vibration*, which made the TMD known to many engineers and scientists [4]. The parameter optimization of the TMD was later investigated in the frequency domain under stationary white noise excitation rather than harmonic excitation [3]. The resulting optimum stiffness and damping factor are similar to those

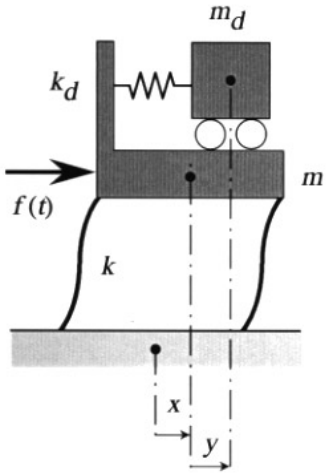

Figure 1. Frahm's original TMD.

obtained under a harmonic excitation. This method was later summarized by Warburton [24], who compared the optimum parameters with different target responses under various excitations.

In the year 1973, the active TMD was first studied by Morison and Karnopp [11], who attempted to improve the vibration control performance by providing an active control force to the device shown in figure 3. They employed the modern control technique and linear quadratic optimum algorithm to obtain an appropriate control command to operate the machine. One of the interesting features of their study is the selection of auxiliary model.

0964-1726/98/410637+17$19.50

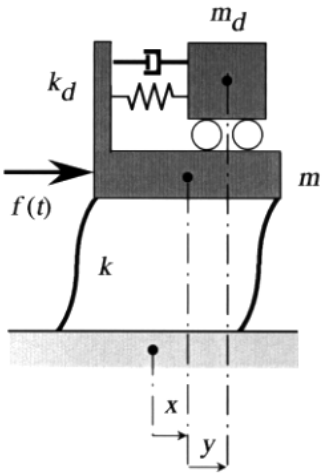

Figure 2. Passive TMD.

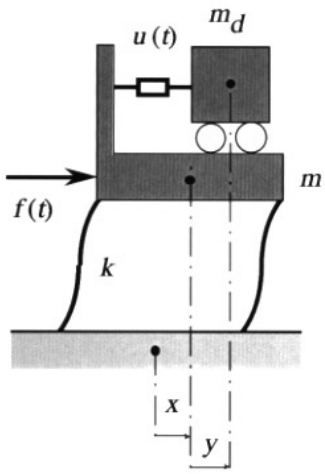

Figure 3. Active mass damper (AMD).

They replaced the damping device and spring by an actuator to generate the required control force and power (figure 4). This method was later called an active mass damper (AMD). When the modern control technique is used to optimize the feedback gains to operate the device, one has no obligation to pay any attention to the original stiffness of the auxiliary mass system. It is, however, important to adjust k_d and c_d of the active TMD for economizing its control force and power. The stiffness of the AMD is comparatively small so that the inertia force created by the motion of the auxiliary mass is roughly linear to the input signal, while the stiffness of the active TMD is adjusted to the tuning stiffness and its natural frequency is close to that of the primary system. The difference between these two different models was later recognized as important to reduce the net control force, power and energy.

In the civil engineering field, the active TMD (figure 4) was first studied by Lund [10] who was one of those engineers working with a project on a TMD that was installed into John Hancock Tower in Boston, followed by another project of City Corp Center in New York city

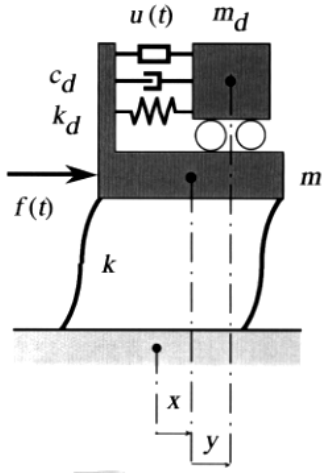

Figure 4. Active TMD.

[12, 19]. Although these projects used the passive TMD principle rather than an active one, hydraulic actuators were used to provide an appropriate damping force to the device. It is true that the algorithm adopted for the projects were merely a passive TMD, yet the system configuration was exactly an active TMD control system. Lund's active TMD study was further extended by Chang and Soong [2], who used the modern control technique to optimize the feedback gain. They selected k_d and c_d as the optimum values derived from the passive TMD formula. This is the first active TMD study in the civil engineering field, though the parameter optimization was not precisely conducted.

As far as civil engineering applications are concerned, methods for the attenuation of structural response under seismic excitation did not receive much attention until the importance was recognized at the time of the *9th WCEE* held at Tokyo and Kyoto in 1988. The steering committee of the conference organized a special theme session under the title of 'Seismic response control of structural systems'. The session highlighted recent developments in seismic response reduction and control methodologies, with emphasis on seismic load reduction, seismic load isolation and response control. This event accelerated application projects of active control in the civil engineering field of Japan, though the emphasis was more focused on wind pressure disturbances rather than ground motion. The first application reported was the work by Kobori [8], followed by others. Since then, there have been numerous works reported with actual application projects [20, 21, 23]. But most of them were related to their own specific devices and their reported results were merely numerical studies obtained by applying the quadratic optimum procedure according to the modern control theory.

In the year 1989, the first application of AMD was completed by Kobori's research team [8]. What made this machine unique was its power supplying hydraulic unit that made the machine start up almost simultaneously when the ground motion occurred. There was a small pump (1.5 kW) working to restore the required energy inside of accumulators in terms of pressure. Once a small earthquake event occurs, another larger pump starts up to

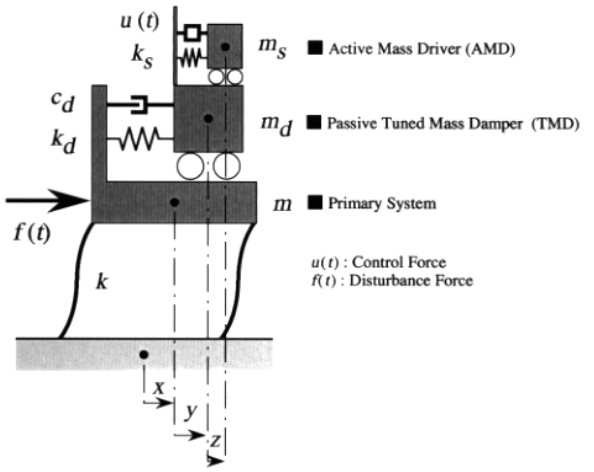

Figure 5. Active–passive composite tuned mass damper.

wind up the actuator to operate the machine, yet it takes time until it goes into full operation. During this transient time, the energy stored inside the accumulator starts pouring into the actuator to compensate the shortage of the power from the main pump system. It is also noted that the algorithm adopted for this controller was velocity feedback and the natural frequency of the secondary system was intentionally away from the first modal frequency of the building model. This active system has been functioning ever since its installation in 1989 except for periodic maintenance checkup occasions.

Most of the aforementioned applications in Japan adopted the auxiliary model studied by Chang and Soong [2]. In fact, the original stiffness of the auxiliary system is adjusted to the 'tuning stiffness' that makes the natural frequency of the secondary system the primary system's first modal frequency. Many people came to notice that the tuning operation could reduce the required control force to some extent. Yet, the damping adjustment and its importance were neither recognized nor optimized. This type of AMD later came to be called a hybrid mass damper (HMD). Those who studied this type of HMD used the modern control method to optimize the feedback gain by crunching out the Riccati equation under the stationary condition.

An interesting relationship between passive and active TMDs was discovered in 1992 by Nishimura [13], who used the acceleration of the primary system as the main feedback gain to optimize the active TMD performance. The principle of the algorithm is briefly reviewed in the following section. The acceleration feedback method clarified the physical meaning of the active TMD operation, and its successfully minimized the auxiliary mass motion, power, force and energy requirement as much as possible.

Independently from these research movements, Yamada [25] submitted an application paper to the Japan Patent Bureau. It was an invention of a composite TMD, which is shown in figure 5. A small mass was actively mounted on a passive TMD, and the motion of the active mass generates inertia force rather than reaction force. Intuitively, this device seemed to work well to attenuate the primary system vibration effectively, yet finding an appropriate algorithm for this complicated machine it far from easy work. After several years dormant research activity, the acceleration feedback method was discovered to be appropriate for creating the control command for the active–passive composite TMD [16]. The method of reducing the necessary control force, power, and energy without degrading its control performance was discovered and it was analytically and experimentally verified under harmonic, stationary random and non-stationary random disturbances.

2. Control algorithm

2.1. Algorithm concept

The control algorithm adopted for the composite TMD is a simple extension of the passive TMD principle. The physical meaning of the algorithm is reviewed as follows [16].

The actively controlled TMD is shown in figure 4, where the control force is introduced between the primary and auxiliary systems by an actuator. First, we consider the equations of motion of the active TMD shown in figure 4.

$$\begin{cases} m_d(\ddot{y} + \ddot{x}) + c_d\dot{y} + k_d y - u(t) \\ m\ddot{x} + kx - c_d\dot{y} - k_d y = -u(t) + mf(t) \end{cases} \tag{1}$$

where m is the mass of the primary system, k the stiffness of the primary system, m_d the mass of the auxiliary system, c_d the damping coefficient of the auxiliary system, k_d the stiffness of the auxiliary system, $f(t)$ the external disturbance, and $u(t)$ is the active control force applied to the TMD. Reconsidering the principle of the passive TMD, the inertia force of the TMD is seen to work as a damping force on the primary system because the TMD motion has approximately 90 degree phase lag behind the motion of the primary system. The incidental disturbance which induces the TMD motion is obviously the acceleration response of the main structure subjected to the external disturbances. Hence, if we could increase the TMD motion linearly, the vibration control effect is expected to increase. This is the basic idea of the acceleration feedback method that is prescribed by

$$u(t) = -mg_a\ddot{x} \qquad \left(g_a < 1.0 \text{ is required for stability}\right). \tag{2}$$

If the feedback gain g_a is zero, the equation of motion represents the passive TMD. Therefore, the parameter optimization of the active TMD according to this control algorithm can be conducted under a harmonic excitation, which is given by

$$f(t) = F\omega_0^2 \exp(\mathrm{i}\omega t). \tag{3}$$

The optimization problem associated with the active TMD is how to select the tuning frequency and damping factor of the auxiliary system. After introducing the

Table 1. Optimum parameters for passive TMD and active TMD under a harmonic excitation.

	Mass ratio μ	Feedback gain g_a	Frequency ratio ξ_{opt}	Damping factor η_{opt}	Response peak α
Passive TMD	0.01	—	0.99	0.06	14.2
Active TMD	0.01	0.20	0.89	0.28	3.0

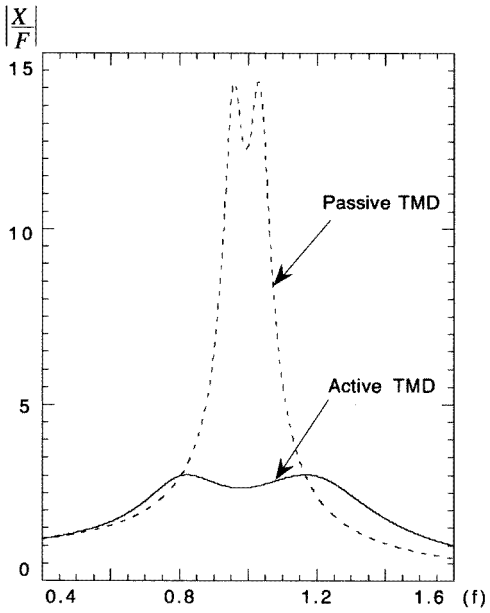

Figure 6. Primary system response.

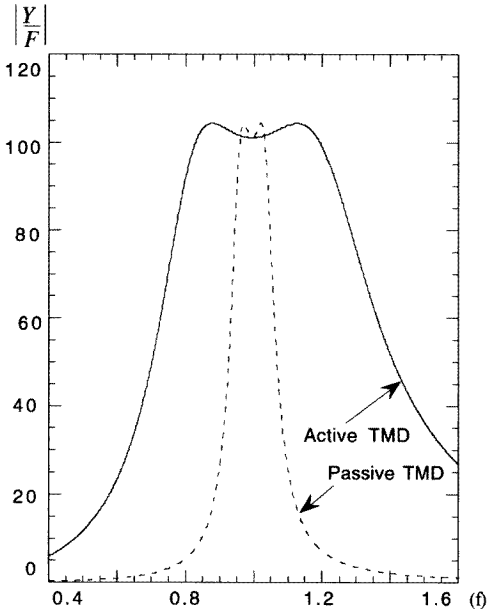

Figure 7. Auxiliary system response.

following notations and substitutions, this parameter optimization is reviewed.

The natural frequency of the TMD: $\omega_d = \sqrt{\dfrac{k_d}{m_d}}$ (4)

The natural frequency of the primal system: $\omega_0 = \sqrt{\dfrac{k}{m}}$ (5)

The mass ratio of the TMD: $\mu = \dfrac{m_d}{m}$ (6)

The frequency ratio of the TMD: $\xi = \dfrac{\omega_d}{\omega_0}$ (7)

The damping factor of the TMD: $\eta = \dfrac{c_d}{2m_d\omega_d}$. (8)

The parameter optimization of the active TMD is exactly the same as the passive TMD optimization [13]. The final results are given below.

The optimum frequency factor: $\xi_{opt} = \dfrac{\sqrt{1-g_a}}{1+\mu}$ or

$$\omega_{opt} = \omega_0\xi_{opt} \text{ or } k_{opt} = m_d\left(\omega_0\xi_{opt}\right)^2 \quad (9)$$

The optimum damping factor: $\eta_{opt} = \sqrt{\dfrac{3(\mu+g_a)}{8(1+\mu)}}$ or

$$c_{opt} = 2m_d\omega_{opt}\eta_{opt}. \quad (10)$$

A numerical calculation is demonstrated to show the difference from the passive TMD. The responses of the primal and auxiliary systems are shown in figures 6 and 7, respectively. The normalized feedback gain g_a is set to 0.2 for the TMD with the mass ratio of 0.01. All the other parameters are calculated and shown in table 1. It is interesting that the peak of the auxiliary system of the active TMD is kept constant regardless of the feedback gain. As a matter of fact, the peak responses of the primary and TMD systems, or equivalently α and β respectively, are given by

$$\alpha = \sqrt{\frac{\mu+2-g_a}{\mu+g_a}} \text{ and } \beta = \frac{1+\mu}{\mu}. \quad (11)$$

Hence, the acceleration feedback method makes it possible to reduce the primal system vibration while the auxiliary system response is restricted as much as possible. (See figures 6 and 7.)

2.2. Parameter optimization under white noise excitation

The optimum parameters of the passive TMD under a white noise excitation were summarized by Warburton [24] who

studied the effect of disturbances on the optimum damping factor and tuning frequency. In this section, the optimum frequency ratio and damping factor for the active TMD are obtained under a white noise excitation.

After substituting (2) into (1), the equations of motion of the active TMD with the acceleration feedback term are converted into the following Laplace transform.

$$\begin{bmatrix} m_d s^2 + c_d s + k_d & (m_d + m g_a)s^2 \\ m_d s^2 & (m_d + m)s^2 + k \end{bmatrix} \begin{bmatrix} Y(s) \\ X(s) \end{bmatrix} = \begin{bmatrix} 0 \\ mF(s) \end{bmatrix}. \tag{12}$$

Hence, the transfer function of $X(s)$ from $F(s)$ is

$$X(s) = H_x(s)F(s) \tag{13}$$

where

$$H_x(s) = s^2 + 2\omega_d \eta s + \omega_d^2 \times \left[(1 - g_a)s^4 + 2(1 + \mu)\omega_d \eta s^3 + (\omega_0^2 + (1 + \mu)\omega_d^2)s^2 + 2\omega_d \omega_0^2 \eta s + \omega_d^2 \omega_0^2\right]^{-1}. \tag{14}$$

The excitation is supposed to be a stationary white noise whose spectral density is S_0. Then the mean square of random variable X under a stationary white noise is given by

$$E\left[X^2\right] = S_0 \int_{-\infty}^{+\infty} H_x(\mathrm{i}\omega) H_x(-\mathrm{i}\omega)\, \mathrm{d}\omega. \tag{15}$$

The evaluation of this integral is carried out in the complex s plane by means of the residue theorem. As a result, we obtain

$$E\left[X^2\right] = \frac{\pi S_0}{2(\mu + g_a)\omega_0^3 \eta}\left[4\xi(1 + \mu)\eta^2 + (1 + \mu)^2 \xi^3 - \left(2 + \mu - g_a\right)\xi + \frac{1}{\xi}\right]. \tag{16}$$

The optimum tuning frequency ratio ξ and damping factor η are the solutions of the next equations.

$$\frac{\partial E[X^2]}{\partial \eta} = 0 \qquad \frac{\partial E[X^2]}{\partial \xi} = 0. \tag{17}$$

Finally, the optimum parameters are obtained as

$$\xi_{opt} = \frac{1}{1 + \mu}\sqrt{\frac{2 + \mu - g_a}{2}} \tag{18}$$

$$\eta_{opt} = \sqrt{\frac{(4 + 3\mu - g_a)(\mu + g_a)}{8(1 + \mu)(2 + \mu - g_a)}}. \tag{19}$$

The final optimum parameters are slightly different from (9) and (10). But the discrepancy between the two formulas is not significant when g_a and μ are small. In the process of parameter optimization described in this section, we are interested in reducing the primary system's displacement response. If we are more concerned about the velocity response of the primary system, we should minimize the velocity response power spectrum density function instead of (16).

$$E\left[\dot{X}^2\right] = \frac{\pi S}{2(\mu + g_a)\omega_0 \eta}\left[(1 + \mu)\xi^3 - 2\left(2\eta^2 - 1\right)\xi + \frac{1}{\xi(1 - g_a)}\right]. \tag{20}$$

Exactly following the same procedure, we obtained the optimum parameters as

$$\xi_{opt} = \sqrt{\frac{1}{1 + \mu}} \tag{21}$$

$$\eta_{opt} = \frac{1}{2}\sqrt{\frac{\mu + g_a}{1 - g_a}}. \tag{22}$$

2.3. Control force minimization under white noise excitation

Considering the physical principle of the control algorithm, we understand that the actuator is supposed to create the driving force which accelerates the motion of the TMD. Then, the stiffness and damping of the TMD are optimized under a white noise excitation. But the stiffness can be realized either by a passive device such as mechanical spring or by a restoring force created by the actuator. It is also possible to provide the optimum damping to the TMD either by a passive viscous material or by a braking force due to the actuator. Hence, it is important to find out a guiding principle to optimize the ratio between the passive and active parameters. Obviously we wish to minimize the net control force without degrading the control effect. Therefore, the control algorithm is modified from (2) to (23) and the net control force is studied under the condition that the total tuning frequency and damping factor are fixed to the optimum values according to (18) and (19) or (21) and (22).

$$u(t) = -m g_a \ddot{x} - g_v \dot{y} - g_d y. \tag{23}$$

The square of the control force is given by

$$[u(t)]^2 = \left[m_d\left(\ddot{x} + \ddot{y}\right) + c_d \dot{y} + k_d y\right]^2. \tag{24}$$

Taking the expected value of both sides of (24) under a white noise excitation, we obtain

$$E\left[U^2\right] = k_d^2 E\left[Y^2\right] + 2k_d m_d E[Y(\ddot{X} + \ddot{Y})] + c_d^2 E\left[\dot{Y}^2\right] + 2c_d m_d E[\dot{Y}\ddot{X}] + m_d^2 E\left[(\ddot{X} + \ddot{Y})^2\right] \tag{25}$$

where X, Y and U are the random variables of x, y and $u(t)$, respectively. The problem here is how to minimize the mean square of the control force. The above equation is just a basic quadratic function in terms of k_d and c_d. Hence, the minimum value is obtained by adjusting k_d and c_d to

$$k_d = -\frac{m_d E[Y(\ddot{X} + \ddot{Y})]}{E[Y^2]} \text{ and } c_d = -\frac{m_d E[\dot{Y}\ddot{X}]}{E[\dot{Y}^2]}. \tag{26}$$

After evaluating these integrals, we finally obtain the optimum parameters and feedback gains as

$$c_d = \frac{\mu}{\mu + g_a} c_{opt} \text{ and } g_v = \frac{g_a}{\mu + g_a} c_{opt} \tag{27}$$

$$k_d = \frac{1}{\mu + g_a}\left(\mu + \frac{g_a}{(1 - g_a)\xi_{opt}^2}\right) k_{opt} \text{ and } g_d = k_{opt} - k_d. \tag{28}$$

It is very important to reduce the net control force and power as much as possible, when the intensity of the disturbance excitation is large. Hence, this control algorithm has a significant advantage when it is applied to a large structure such as a tall building subjected to wind turbulence or earthquake ground motion, because the control force and power are substantially reduced without degrading vibration control effect.

2.4. Control power minimization under white noise excitation

In the previous sections, we minimized the net control force without degrading the performance under a white noise excitation. In this section, we aim to eliminate the control power in an average sense under a white noise excitation. After multiplying the velocity vector from the left-hand side of (1), we obtain the power equilibrium such as

$$m\dot{x}\ddot{x} + k\dot{x}x + m_d(\dot{x}+\dot{y})(\ddot{x}+\ddot{y}) + k_d\dot{y}y + c_d(\dot{y})^2 - \dot{y}u(t) = m\dot{x}f(t). \tag{29}$$

The disturbance excitation is supposed to be a stationary white noise and all the responses are replaced by random variables. After taking the expected value of both sides of (29), we obtain

$$c_d E[\dot{Y}^2] = E[\dot{Y}U] + mE[\dot{X}F] \tag{30}$$

where X, Y, U and F are the random variables of x, y, u and $f(t)$, respectively. If we could select c_d in such a manner that the control power, the first term of the right-hand side of (30), in an ensemble sense could be zero, this c_d would be the optimum value. Hence, the optimum damping coefficient is given by

$$c_d = \frac{mE[\dot{X}F]}{E[\dot{Y}^2]} \text{ or equivalently } E[\dot{Y}U] = 0. \tag{31}$$

The numerator of the above equation is obtained by calculating the impulse response of the system, and the denominator is evaluated by the power spectra density in the frequency domain. The final results are shown below.

$$E[\dot{X}F] = \frac{\pi S_0}{1-g_a} \tag{32}$$

$$E[\dot{Y}^2] = \left(\frac{1}{1-g_a}\right)\left(\frac{\mu+g_a}{\mu}\right)\left(\frac{\pi S_0}{2\mu\omega_d\eta_{opt}}\right). \tag{33}$$

Substitution of (32) and (33) into (31) yields

$$c_d = \frac{\mu}{\mu+g_a}c_{opt}. \tag{34}$$

Hence, the rest of the optimum damping should be generated by the actuator, which means that the feedback gain g_v should be

$$g_v = \frac{g_a}{\mu+g_a}c_{opt} \tag{35}$$

which is identical to (27). Interestingly, two different definitions yield the identical solution for the passive damping coefficient and the active velocity feedback gain. Hence, the optimum solution minimizes not only the control force but also the control power under a white noise excitation. The optimum solution that minimizes the control force under a harmonic excitation was discussed and obtained by the present authors, and exactly the same solution was achieved [13]. Hence, the three different definitions for optimizing the passive and active parameters yielded the same solution. In the following section, the statistically predicted control performance is numerically evaluated in the time domain under non-stationary random excitations.

2.5. Control power minimization under random excitation

Under earthquakes or wind gusts, there is a question as to the validity of (27) and (34) which are obtained under a stationary random excitation. In this section, the statistically expected power equilibrium is discussed in a deterministic sense under non-stationary random excitation. Taking the integrals of both sides of (1), we can evaluate the energy equilibrium over a long period of time. Finally, the energy equilibrium is given by

$$\frac{1}{2}m\dot{x}^2 + \frac{1}{2}kx^2 + \frac{1}{2}m_d(\dot{x}+\dot{y})^2 + \frac{1}{2}k_d y^2 + c_d\int_0^T(\dot{y})^2\,\mathrm{d}t - \int_0^T \dot{y}u(t)\,\mathrm{d}t = m\int_0^T \dot{x}f(t)\,\mathrm{d}t \tag{36}$$

where T is a certain time after the event of disturbance excitation of $f(t)$. As the time T goes to infinity, the kinetic energies of both the primal system and the TMD converge to zero. Hence, the energy equilibrium at the final stage of the disturbance event should satisfy

$$c_d\int_0^\infty(\dot{y})^2\,\mathrm{d}t - \int_0^\infty \dot{y}u(t)\,\mathrm{d}t = m\int_0^\infty \dot{x}f(t)\,\mathrm{d}t. \tag{37}$$

If the disturbance excitation is known in advance, we can calculate the responses in the time domain, because the optimum total damping coefficient and stiffness are determined by the formulas according to (9) and (10) or (18) and (19). Hence, it is natural to define the passive optimum damping coefficient by

$$c_d = \frac{m\int_0^\infty \dot{x}f(t)\,\mathrm{d}t}{\int_0^\infty(\dot{y})^2\,\mathrm{d}t} \text{ or equivalently } \int_0^\infty \dot{y}u(t)\,\mathrm{d}t = 0. \tag{38}$$

The rest of the damping should be generated by the actuator whose feedback gain g_v is to be $(c_{opt} - c_d)$. If and only if the passive damping is selected as the value given by (38), the control energy converges to zero at the final stage of the disturbance excitation. Therefore, the optimum passive damping coefficient is defined by (38), which eliminates the control energy as the time goes to infinity. It is, however, impossible to know the exact disturbance earthquakes or wind gusts before they actually happen. This is the limitation of the deterministic approach. As we discussed in the previous sections, if the disturbance is supposed to be a white noise, this optimum passive damping factor makes the control power zero at any time in an ensemble sense. In this section, the statistically predicted

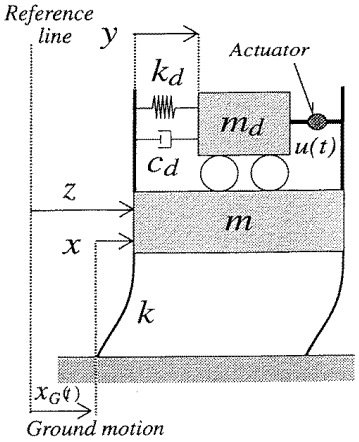

Figure 8. Active TMD under earthquake excitation.

c_d and g_v are numerically evaluated under earthquake ground motion to see whether (38) is satisfied or not. First, the total system subjected to an earthquake motion is shown in figure 8, from which we obtain the equations of motion as

$$\begin{cases} m_d(\ddot{z}+\ddot{y}) + c_d\dot{y} + k_d y = u(t) \\ m\ddot{z} + kz - c_d\dot{y} - k_d y = -u(t) + kx_G \end{cases} \tag{39}$$

where z, x_G are the absolute displacement response of the primal system and ground motion, respectively. The whole derivation of the formulas is invariant, if we feed back the absolute acceleration of the primal system instead of the relative value. Hence, the control algorithm should be

$$u(t) = -mg_a\left(\ddot{x}+\ddot{x}_G\right) - g_v\dot{y} - g_d y. \tag{40}$$

One of the advantages of the control algorithm of (40) is that the sensing equipment and control signal processing are not influenced by the types of disturbance. In fact, the acceleration sensor attached at the top of the primal system detects its absolute motion whether it is subjected to earthquakes or wind turbulences.

An example calculation is carried out to evaluate the energy equilibrium predicted in a probabilistic sense under an earthquake excitation. The energy equilibrium is obtained by multiplying the velocity vector from the left-hand side of (39). The final result is

$$E_s + E_t + E_d = E_c + E_i \tag{41}$$

where

$$\text{structure energy: } E_s = \tfrac{1}{2}m[\dot{x}(t)]^2 + \tfrac{1}{2}k[x(t)]^2 \tag{42}$$

$$\text{TMD energy: } E_t = \tfrac{1}{2}m_d[\dot{x}(t)+\dot{y}(t)]^2 + \tfrac{1}{2}k_d[y(t)]^2 \tag{43}$$

$$\text{passive damper energy: } E_d = c_d\int_0^t [\dot{y}(\tau)]^2\,\mathrm{d}\tau \tag{44}$$

$$\text{control cumulative energy: } E_c = \int_0^t \dot{y}(\tau)u(\tau)\,\mathrm{d}\tau \tag{45}$$

$$\text{input energy due to earthquake: } E_i = -\int_0^t \left[\left(m+m_d\right)\dot{x}(\tau) + m_d\dot{y}(\tau)\right]\ddot{x}_g(\tau)\,\mathrm{d}\tau. \tag{46}$$

Table 2. Optimum parameters and feedback gains for an example analysis under an earthquake excitation.

	Notations	Values
Primary system parameters	m (kg)	9.80×10^5
	k (N m^{-1})	3.87×10^7
	ω_0 (rad s^{-1})	6.28
Mass parameters	m_d (kg)	9.80×10^3
	μ	0.01
	g_a	0.03
Stiffness parameters	k_d (N m^{-1})	3.80×10^5
	g_d (N m^{-1})	-0.23×10^5
Damping parameters	c_d (N s^{-1} m^{-1})	0.36×10^4
	g_d (N s^{-1} m^{-1})	1.06×10^4

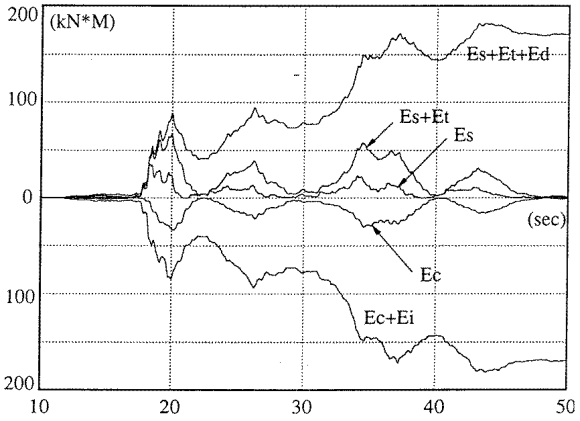

Figure 9. Energy time history under Hachinohe (NS) earthquake. (Control energy, E_c, converges to null as the time goes to infinity.)

The disturbance excitation for this study is the Hachinohe (NS) earthquake whose peak acceleration is scaled down to 100 cm s^{-2}. The mass ratio μ is set to 0.01, while the normalized feedback gain g_a is 0.03. The other parameters are determined according to (27), (28), (34) and (35). All the parameters and feedback gains are given in table 2. It is to be noted that the control energy converges to zero at the final stage of the disturbance excitation, as is predicted in the statistic analysis. Though there is only one analytical solution shown in this paper, yet numerous analyses have been conducted to verify the relation (38) under different earthquakes and all of the results support the fact that the control energy converges to zero as the time goes to infinity under any non-stationary random excitations [16]. As is shown in figure 9, the whole input energy brought by the earthquake into the total system is dissipated by the passive damping material, and the cumulative control energy due to the actuator converges to zero.

2.6. Replacement of the sensors by a state estimator

An attractive feature of the acceleration feedback method is that we need only one single sensor to create the command signal to operate the actuator. If we wish to reduce the control power, force and energy, we need two additional sensors to detect the TMD motion. Naturally, we wish

to design a state estimator to eliminate these additional sensors. In this section, a state estimator expressed in a transfer function is discussed on condition that all the passive parameters of the TMD are precisely identified or fixed to the appropriate values.

The whole derivation of the optimum formulas is not altered, except that the normalized feedback gain is no longer a constant but is a filter expressed in (49).

$$\begin{cases} m_d\ddot{y} + c_d\dot{y} + k_d y = -m_d\ddot{x} + u(t) \\ (m_d + m)\ddot{x} + kx = f(t) - m_d\ddot{y} \end{cases} \tag{47}$$

$$u(s) = -mg(s)\ddot{x}(s) \tag{48}$$

$$g(s) = \left(\frac{m_d s^2 + c_d s + k_d}{m_d s^2 + c_{opt} s + k_{opt}}\right)(g_a + \mu) - \mu. \tag{49}$$

Expressing the above equations in the time domain, we can retrieve the equation of motion given below

$$\begin{cases} m_d\ddot{y} + c_{opt}\dot{y} + k_{opt} y = -m_d\ddot{x} + u(t) \\ (m_d + m)\ddot{x} + kx = f(t) - m_d\ddot{y} \\ u(t) = -mg_a\ddot{x} \end{cases} \tag{50}$$

which is identical to (1) with the algorithm (2). Hence, we can substitute the displacement and velocity sensors by the filtered version of the feedback gain by (49). It is also noted that the passive parameter c_d should be selected as the desirable value given by (27) so that the control power and force are minimized. Reviewing the derivation of the control force and power minimization under white noise excitation and the control energy minimization under a non-stationary random excitation, the optimum passive parameters are not influenced at all because the whole derivation does not contain the algorithm explicitly. As long as the response of the primary and auxiliary systems are invariant, the optimum passive parameter c_d is still given by

$$c_d = \frac{\mu}{\mu + g_a} c_{opt}. \tag{51}$$

If the passive damping coefficient c_d is selected as the above value, the filtered feedback gain is obtained after substituting (51) into (49).

$$g(s) = \frac{g_a(s^2 + \omega_d^2) + \mu(\omega_d^2 - \omega_{opt}^2)}{s^2 + 2\omega_{opt}\eta_{opt}s + \omega_{opt}^2}. \tag{52}$$

If and only if the passive damping coefficient c_d is selected as the value prescribed by (51), the filtered version of feedback gain becomes a notch-filter whose null point is close to ω_d. This is the physical meaning of why the control force becomes smaller if the tuning frequency is close to the primary system's natural frequency. It is also to be noted that the optimum passive damping coefficient c_d is not influenced by the spectrum of the disturbance excitation while the optimum passive stiffness k_d depends on the external disturbance excitation.

One of the advantages of the filtered feedback gain or equivalently a state estimator expressed in the transfer function is that we are able to adjust the TMD frequency to a desired optimum value after the device is settled on the target building structure. This is a solution to an inherent weak point associated with the TMD device. Once an actual device is implemented on the structure, it is quite difficult to adjust its stiffness to obtain the maximum control performance. If it is possible to adjust the device stiffness not mechanically but electrically, it would be a significant advantage from a practical point of view.

In fact, the proposed filtered feedback gain suggests the possibility of tuning adjustment after installation. It is also noted that the optimum passive damping coefficient c_d is not influenced by this tuning adjustment. Hence, the energy equilibrium achieved by the acceleration feedback strategy is not violated by applying the filtered feedback gain. This reasoning reaches to the extension of the acceleration feedback method to a multi-modal control algorithm.

2.7. Extension to a multi-degree-of-freedom model

A real building structure is a multi-degree-of-freedom model rather than a simple lumped mass model. Hence, we must slightly modify the set of formulas obtained for a single-degree-of-freedom model into another version that is applicable to a more complex structure model. Once a target structure model is expressed in a matrix form, then we can expand it into discrete mode vectors. Once this task is finished, we can calculate the effective modal mass associated with the control vector that is corresponding to the location of TMD. Based on the identified modal effective mass, it is now possible to evaluate the TMD mass ratio and to normalize the feedback gain. In this section, an example model is used for demonstrating how to apply the aforementioned optimum formulas to an actual structural model for achieving the equivalent control performance obtained for a single-degree-of-freedom model.

An imaginary 4DOF model shown in figure 10 is a target structure onto the top of which an active TMD is implemented. There are lateral shear springs between the neighboring mass points that represent their floor weights and locations. The inherent damping coefficient associated with this original model is assumed to be zero. An eigenvalue analysis is conducted to obtain the first modal effective mass and modal vector so that we can reduce the model into a single-degree-of-freedom model. The result of eigenvalue analysis is shown in figure 10 from which the effective modal mass, mass ratio, normalized feedback gain and the optimum parameters are all obtained.

After reducing the 4DOF model to an SDOF model shown in figure 10, we can obtain the following equation of motion associated with the first mode vibration of the original model.

$$\begin{cases} m_d\ddot{y} + c_{opt}\dot{y} + k_{opt} y = -m_d\ddot{x}_1 + u(t) \\ (m_d + m_1)\ddot{x}_1 + k_1 x_1 = f_1(t) - m_d\ddot{y} \\ u(t) = -m_1 g_{1,a}\ddot{x}_1. \end{cases} \tag{53}$$

One of the important issues associated with a multi-degree-of-freedom model is whether the system stability is influenced by any higher modes. The stability criterion for the acceleration feedback is very simple: the normalized feedback gain g_a should not be greater than 1.0. This statement holds its validity for higher mode criteria as well,

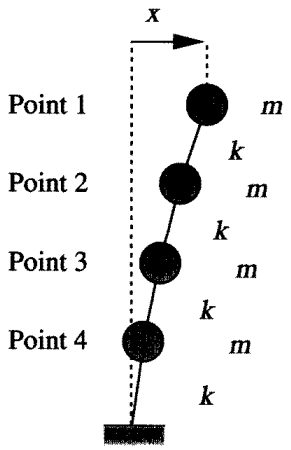

	Eigen Vectors			
{u}	1st mode	2nd mode	3rd mode	4th mode
u_1	1.0000	1.000	1.0000	1.0000
u_2	0.8794	0.000	-1.3473	-2.5321
u_3	0.6527	-1.000	-0.5321	2.8296
u_4	0.3473	-1.000	1.5321	-1.8796

The TMD is placed at point 1 . All the modal vectors in the table above are normalized in such a manner that the corresponding element is caled to unit value or 1.0.

	1st mode	2nd mode	3rd mode	4th mode
ω_i (r/s)	0.3473	1.0	1.5321	1.8794
m_i	2.320	3.00	5.446	18.951
k_i	0.2798	3.00	12.78	66.94

ω_i : circular angle frequency for i-th mode [unit is $\omega_o = \sqrt{\frac{k}{m}}$]

k_i : effective modal stiffness associated with the control vector [unit is k]

m_i : effective modal mass associated with the control vector [unit is m]

m_i is obtained by $m_i = \sum_{j=1}^{4} (u)_j^2$

Figure 10. Reduction of 4DOF model into SDOF model.

because it does not include any information about either TMD parameter or system frequency. Once we precisely identify the higher modal masses associated with the control vector that corresponds to the TMD location, then we can convert the feedback gain into normalized feedback gain with respect to each higher mode. As a result, we can easily evaluate the stability of the acceleration feedback method with respect to any higher mode. For example, if the feedback gain is $1.0m$, the normalized feedback gain with respect to the first mode, $g_{1,a}$, is 0.431 because the modal mass associated with the first mode is $2.32m$. In contrast, the modal mass associated with the second mode is $3.00m$ so that the feedback gain normalized with respect to the second mode, $g_{2,a}$, is 0.333, which is less than the normalized feedback gain with respect to the first mode. Hence, this feedback gain is also stable for the second mode. In fact, any higher modal mass associated with the control vector corresponding to this TMD location (see point 1 in figure 10) is greater than the first modal mass. This statement certifies this acceleration feedback gain, $1.0m$, is stable for any higher modes.

The rest of this problem of creating the acceleration feedback signal is how to discrete the primary mode response from other higher mode contamination. If we place one accelerometer at point 1, the signal from the sensor contains higher mode responses as well as the first

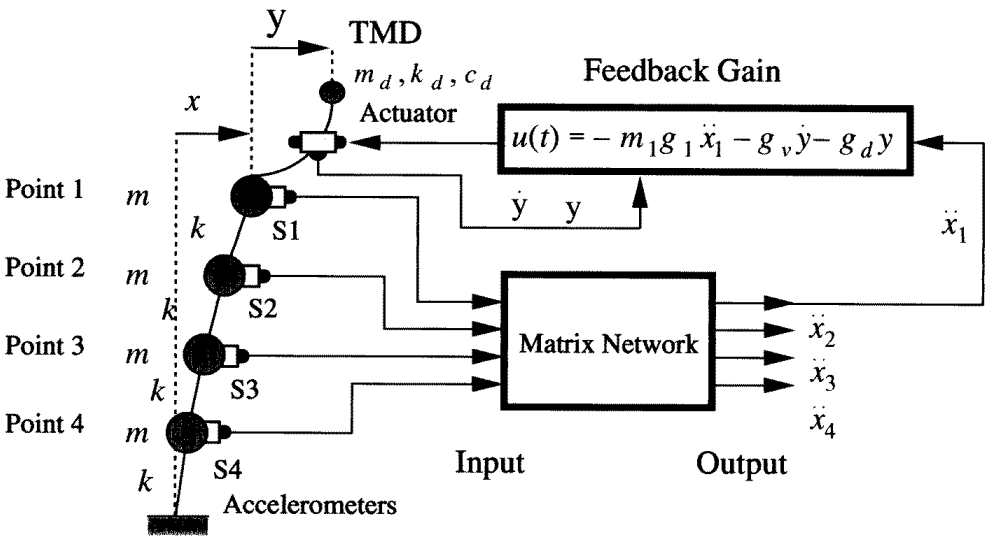

Sensing Network

$$\begin{pmatrix} \ddot{X}_1 \\ \ddot{X}_2 \\ \ddot{X}_3 \\ \ddot{X}_4 \end{pmatrix} = \begin{pmatrix} 0.43178 & 0.3719 & 0.28346 & 0.14832 \\ 0.33246 & 0.00221 & -0.33585 & -0.33169 \\ 0.18338 & -0.24677 & -0.09843 & 0.28182 \\ 0.05238 & -0.13263 & 0.15082 & -0.09844 \end{pmatrix} \begin{pmatrix} \ddot{S}_1 \\ \ddot{S}_2 \\ \ddot{S}_3 \\ \ddot{S}_4 \end{pmatrix}$$

Acceleration Feedback Algorithm for 4 DOF Model

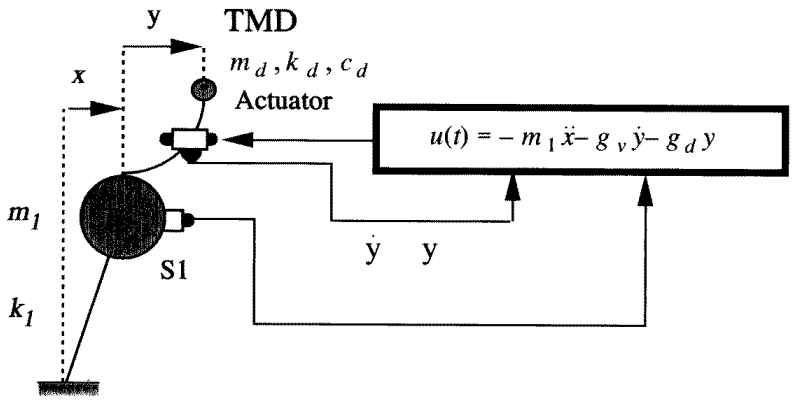

Acceleration Feedback Algorithm for the Equivalent SDOF Model

Figure 11. Sensing network and feedback gain for a multi-degree-of-freedom model and equivalent single-degree-of-freedom model.

mode component. It is extremely difficult to extract the primary mode component from the original signal, because the higher mode frequencies are not far enough away from the first mode frequency. In addition to this, any filtering operation results in some phase lag at the target frequency and it deteriorates the control performance.

The only possible method to select primary acceleration from the 4DOF model is to use four sensors; each point has one accelerometer to take the source signal. Then this source signal is put through a matrix network to separate the four modal responses. This purification or discrete process is made possible by applying the modal expansion

theorem. The conceptual idea is shown in figure 11. The matrix network is a simple linear transformation which is the inverse matrix of the eigenmatrix as follows.

$$\begin{pmatrix} X_1 \\ X_2 \\ X_3 \\ X_4 \end{pmatrix} = \begin{pmatrix} 1 & 1 & 1 & 1 \\ 0.8794 & 0.0 & -1.3473 & -2.5321 \\ 0.6527 & -1.0 & -0.5321 & 2.8296 \\ 0.3473 & -1.0 & 1.5321 & -1.8796 \end{pmatrix}^{-1} \begin{pmatrix} S_1 \\ S_2 \\ S_3 \\ S_4 \end{pmatrix} = \begin{pmatrix} 0.43178 & 0.37719 & 0.28346 & 0.14832 \\ 0.33246 & 0.00221 & -0.33585 & -0.33169 \\ 0.18338 & -0.24677 & -0.09843 & 0.28182 \\ 0.05238 & -0.13263 & 0.15082 & -0.09844 \end{pmatrix} \times \begin{pmatrix} S_1 \\ S_2 \\ S_3 \\ S_4 \end{pmatrix} \tag{54}$$

where X_i is the discrete ith mode signal normalized with respect to point i and S_i the raw signal from point i in terms of absolute acceleration.

An example numerical calculation is conducted to certify the identity of the reduced SDOF model with the original 4DOF model shown in figure 12. The external disturbance is El Centro (NS) ground motion with the peak acceleration of 100 cm s^{-2}. One thing to be noted is that the effective first modal mass is about 35% of the total mass of the 4DOF model but the input ground motion should be multiplied by the participation coefficient factor, in this particular case 1.23, so that the input energy into the SDOF model by the same earthquake can be equalized to the input energy of the 4DOF model.

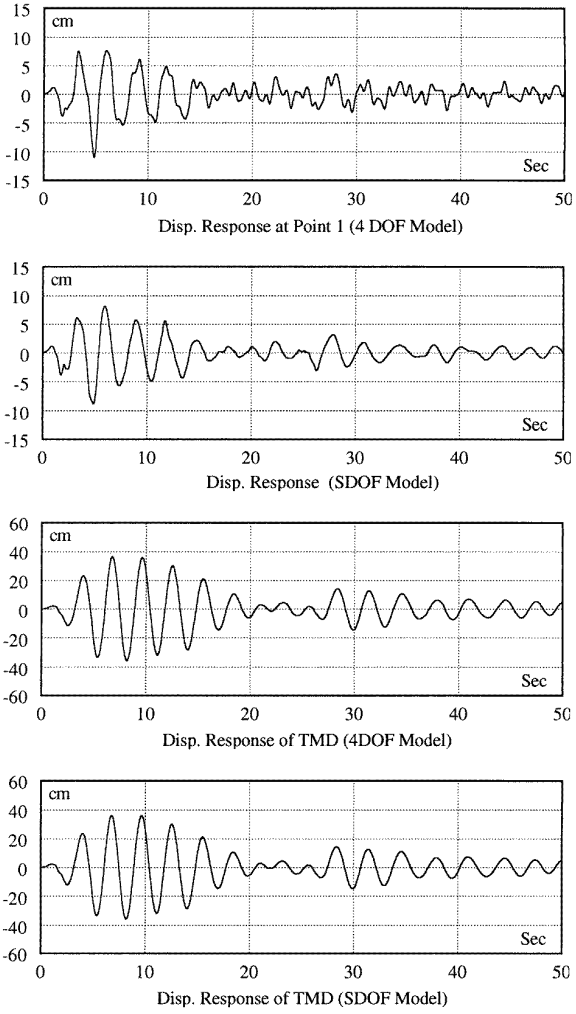

Figure 12. Comparison of SDOF reduced model with the original 4DOF model.

2.8. Higher mode vibration control

If we wish to subdue the second mode response vibration as well as the first mode, we could design an active TMD according to the aforementioned procedure in the previous section. The second modal mass, m_2, associated with the TMD location (point 1) has already been obtained and shown in figure 10. Hence, the equation of motion with respect to the second mode response is given below.

$$\begin{cases} m_d\ddot{y} + c_{opt}\dot{y} + k_{opt}y = -m_d\ddot{x}_2 + u(t) \\ (m_d + m_2)\ddot{x}_2 + k_2x_2 = f_2(t) - m_d\ddot{y} \\ u(t) = -m_2g_{2,a}\ddot{x}_2. \end{cases} \tag{55}$$

The sensing technique is also identical to the matrix network by (54), which means that any higher mode control is possible. Yet, the most appropriate TMD location varies according to the target mode. Obviously, the optimum stiffness and damping factor are different from the first mode's optimum values. Therefore, the designed active TMD is totally different from the first mode active TMD. It is true that this is a rather discouraging result, but there is a way to make the active TMD effective for both first mode and second mode simultaneously. The state estimator or equivalently the filtered version of the feedback gain in (49) makes it possible to adjust the active TMD stiffness electrically in spite of its mechanical stiffness. Just a little extension of the filtered version feedback gain makes it possible to control the first and second modes simultaneously by a single active TMD placed at point 1. The control algorithm concept is shown in figure 13. The control feedback algorithm is explicitly given below by referring to the sensing network in figure 11.

$$\begin{aligned} u(s) = &-m_1g_1(s)\big(0.43178S_1 + 0.37719S_2 + 0.28346S_3 \\ &+0.14832S_4\big) \\ &-m_2g_2(s)\big(0.33246S_1 + 0.00221S_2 - 0.33585S_3 \\ &-0.33169S_4\big) \end{aligned} \tag{56}$$

where

$$g_1(s) = \left(\frac{m_ds^2 + c_ds + k_d}{m_ds^2 + c_{1,opt}s + k_{1,opt}}\right)\big(g_{1,a} + \mu_1\big) - \mu_1 \tag{57}$$

$$g_2(s) = \left(\frac{m_ds^2 + c_ds + k_d}{m_ds^2 + c_{2,opt}s + k_{2,opt}}\right)\big(g_{2,a} + \mu_2\big) - \mu_2. \tag{58}$$

The analytical results are shown in figure 14 from which we understand the second mode response is subdued as well

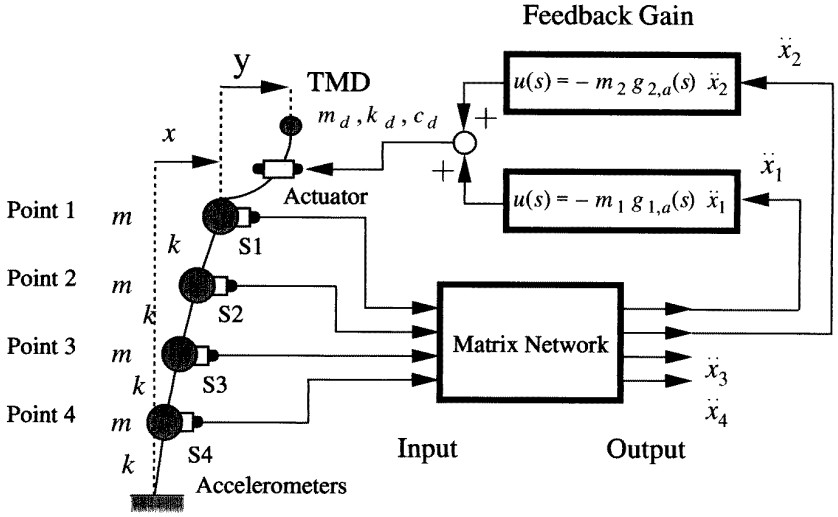

Sensing Network

$$\begin{pmatrix} X_1 \\ X_2 \\ X_3 \\ X_4 \end{pmatrix} = \begin{pmatrix} 0.43178 & 0.37719 & 0.28346 & 0.14832 \\ 0.33246 & 0.00221 & -0.33585 & -0.33169 \\ 0.18338 & -0.24677 & -0.09843 & 0.28182 \\ 0.05238 & -0.13263 & 0.15082 & -0.09844 \end{pmatrix} \begin{pmatrix} S_1 \\ S_2 \\ S_3 \\ S_4 \end{pmatrix}$$

Filtered Feedback Gain

$$g_{1,a}(s) = \frac{m_d s^2 + c_d s + k_d}{m_d s^2 + c_{opt,1} s + k_{opt,1}} (g_{1,a} + \mu_1) - \mu_1$$

$$g_{2,a}(s) = \frac{m_d s^2 + c_d s + k_d}{m_d s^2 + c_{opt,2} s + k_{opt,2}} (g_{2,a} + \mu_2) - \mu_2$$

where $\mu_1 = \frac{m_d}{m_1}$ $\mu_2 = \frac{m_d}{m_2}$

Figure 13. Sensing network and feedback gain for a multi-modal control algorithm.

Table 3. Mathematical model for the project frame structure. (The original model is a 14-degree-of-freedom model.)

	X-direction			*Y*-direction	
	Effective mass	1010 MT		Effective mass	1010 MT
First	Frequency	1.23 s	First	Frequency	1.26 s
mode	Modal damping	1.0%	mode	Modal damping	1.0%

as the first mode by the algorithm shown above. Any higher mode response control is possible by extending the same algorithm into the target mode. If you wish to control the third mode response as well, it would be recommended to place the active TMD at point 4 where the corresponding component of the third modal vector is maximum, because the effective third modal mass associated with the control vector is much less than obtained otherwise. It you wish to use the same active TMD placed at point 1 for third mode vibration control, it would be, of course, possible. But there are several factors to be considered before determining the control performance. The normalized feedback gain should be less than 0.426, because the effective modal mass for the first mode is 2.73*m* while the effective modal mass for the third mode is 5.466*m*. Therefore, the system stability would be violated if the normalized feedback gain with respect to the third mode were larger than 0.426. Hence, the control performance with respect to the third mode will

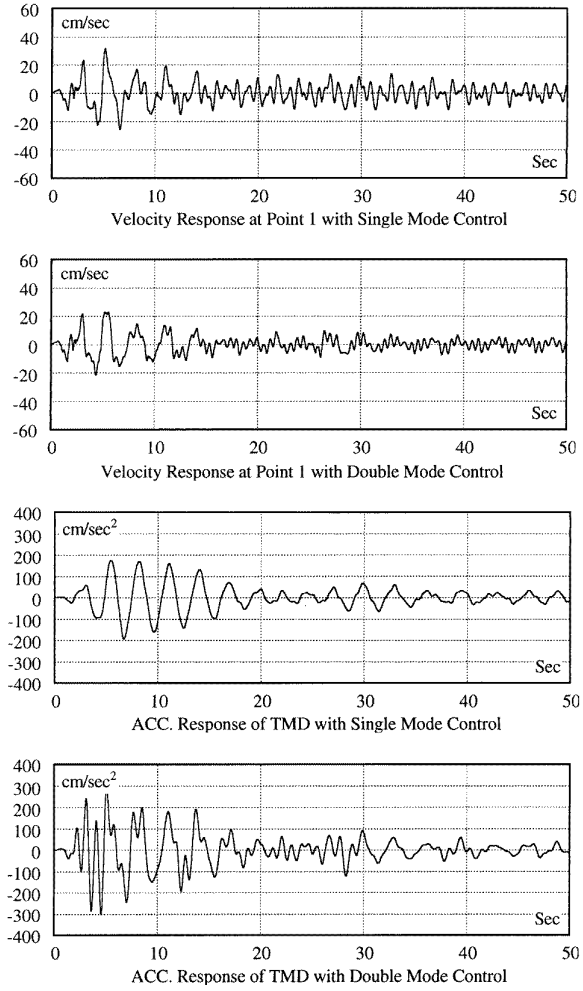

Figure 14. Comparison of double-mode control and single-mode control (4DOF Model under El Centro NS excitation with 0.1 *g* acceleration).

be significantly small because the third mode is not easily controlled by the active TMD placed at point 1.

The same algorithm is easily extended into various types of acceleration feedback strategy. One example is the full mode feedback operation illustrated in figure 15. Another example is a coupled active TMD to reduce the lateral and torsional responses simultaneously shown in figure 16. Depending on the demands of application projects, you could extend the same acceleration feedback strategy into the actual design of the device. Even if the final system configuration is complicated, the basic physical meaning of the device operation is so clear that you will be able to achieve the theoretically verified control performance without difficulty from the actual machine.

2.9. Replacement of reaction force by inertia force

The feasibility of the active TMD is substantially increased by the invention of a composite TMD (figure 1), because the active portion of the control device is significantly decreased, which reduces the total expenditure on the device fabrication. The problem to be discussed is how to operate this complicated machine effectively. In this section, the relation between the acceleration feedback method and the composite TMD is discussed.

If we could produce the net control force by means of the inertia force associated with the secondary mass mounted on the passive TMD, the whole derivation of formulas given in the previous sections would not be altered [17]. The optimization of the parameters, minimization of control force and power and reduction of auxiliary mass motion are all satisfied simultaneously under various types of excitation just like the way proved in the previous sections. In an application, however, the dynamics of the secondary mass is also an important factor for the design. The stiffness and damping of the active portion is also carefully selected. One of the appropriate choices is a relatively low stiffness and damping factor, because the net control force can be approximated by the command control force applied between the passive portion and active mass. Another possibility is that the active mass is also tuned to the natural period of the building structure. Therefore, the phase response of the active mass is at approximately 90° with respect to the input command control force. In other words, the secondary mass system works as a differentiator. This algorithm was numerically studied and experimentally evaluated by the present authors [14]. For details of this type of device design the reader should refer to Koshika [9]. A brief explanation of an application project using the acceleration feedback algorithm is given in the following section.

3. Application

A project using the algorithm along with the concept of the composite TMD started in 1991. The target office building under the design process at that time is shown in figure 17. The total weight of the 14 story high building is approximately 2600 MT; the first modal period is approximately 1.3 s in both lateral directions. It was expected that this target structure was susceptible to wind pressures to induce response motions which might degrade the serviceability of the office space. The requirement from the client motivated an improved mass damper project reported herein.

Even though the total weight of the structure is 2600 MT, the effective first modal mass associated with the control vector, which corresponds to the controller's location, is approximately 1010 MT in both directions. Hence the mass ratio for this composite TMD was selected as 2% and the normalized feedback gain was designed as 10%. As a result of this feedback gain and original mass ratio, the expected damping augmentation is about 10%. Considering these design criteria, we determined the composite TMD's configuration: the TMD weight is 20 MT and two identical active mass drivers (AMDs) are mounted on it so that the lateral motions in both directions are subdued to an insensible level during wind pressure disturbances.

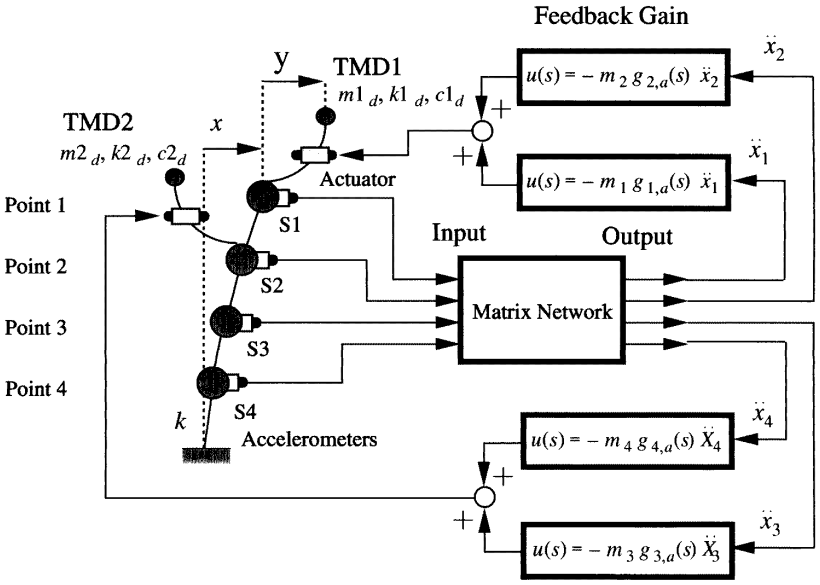

Sensing Network

$$\begin{pmatrix} X_1 \\ X_2 \\ X_3 \\ X_4 \end{pmatrix} = \begin{pmatrix} 0.43178 & 0.37719 & 0.28346 & 0.14832 \\ 0.33246 & 0.00221 & -0.33585 & -0.33169 \\ -0.24707 & 0.33247 & 0.13262 & -0.37969 \\ -0.13263 & 0.33583 & -0.38189 & 0.24926 \end{pmatrix} \begin{pmatrix} S_1 \\ S_2 \\ S_3 \\ S_4 \end{pmatrix}$$

Filtered Feedback Gain

$$g_{1,a}(s) = \frac{m1_d s^2 + c1_d s + k1_d}{m1_d s^2 + c_{1,opt} s + k_{1,opt}} (g_{1,a} + \mu_1) - \mu_1$$

$$g_{2,a}(s) = \frac{m1_d s^2 + c1_d s + k1_d}{m1_d s^2 + c_{2,opt} s + k_{2,opt}} (g_{2,a} + \mu_2) - \mu_2$$

$$g_{3,a}(s) = \frac{m2_d s^2 + c2_d s + k2_d}{m2_d s^2 + c_{3,opt} s + k_{3,opt}} (g_{3,a} + \mu_3) - \mu_3$$

$$g_{4,a}(s) = \frac{m2_d s^2 + c2_d s + k2_d}{m2_d s^2 + c_{4,opt} s + k_{4,opt}} (g_{4,a} + \mu_4) - \mu_4$$

where $m_1 = 2.32\ m$; $m_2 = 3.0\ m$; $m_3 = 3.0\ m$; $m_4 = 2.96\ m$

Figure 15. Sensing network and feedback gain for a multi-mode control algorithm.

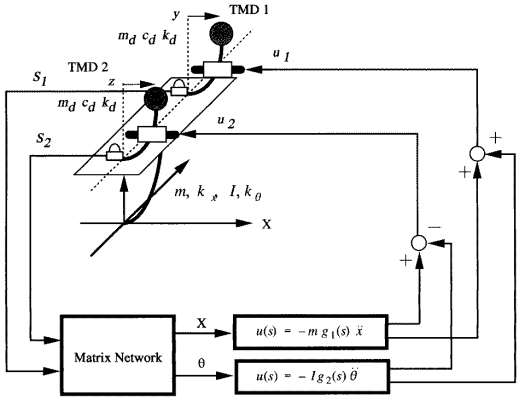

Figure 16. Illustration of lateral and torsional mode control.

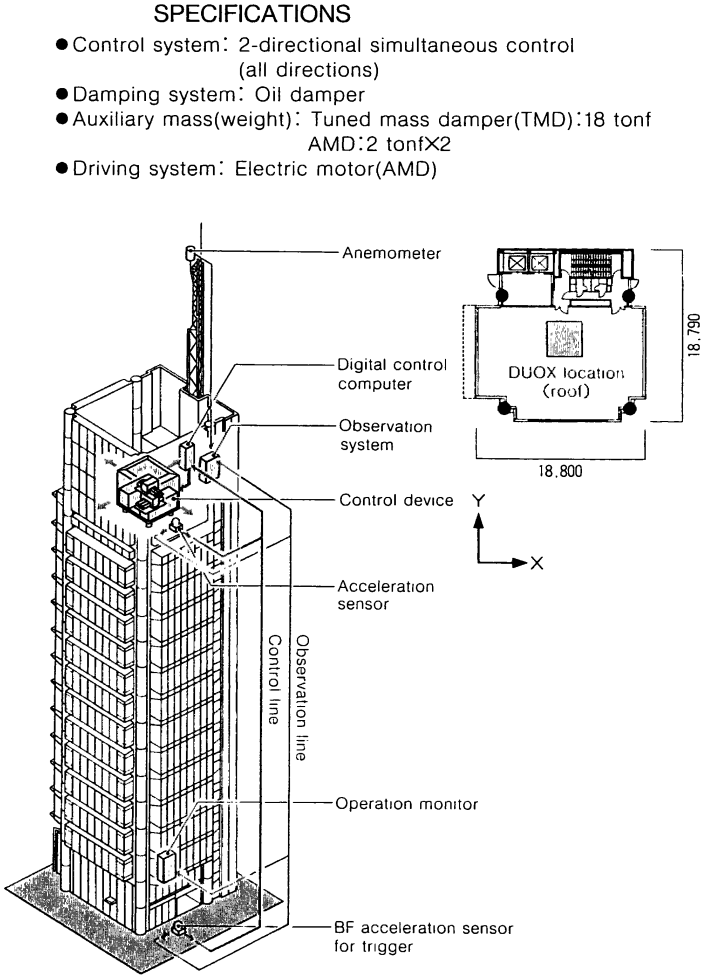

Figure 17. Installation of the composite TMD into an office building.

SPECIFICATIONS
● Control system: 2-directional simultaneous control
(all directions)
● Damping system: Oil damper
● Auxiliary mass(weight): Tuned mass damper(TMD):18 tonf
AMD:2 tonfX2
● Driving system: Electric motor(AMD)

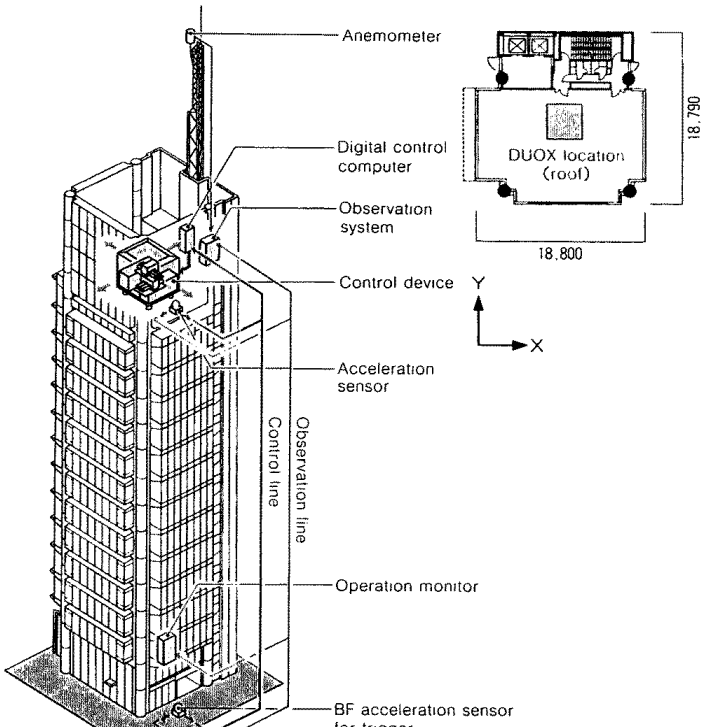

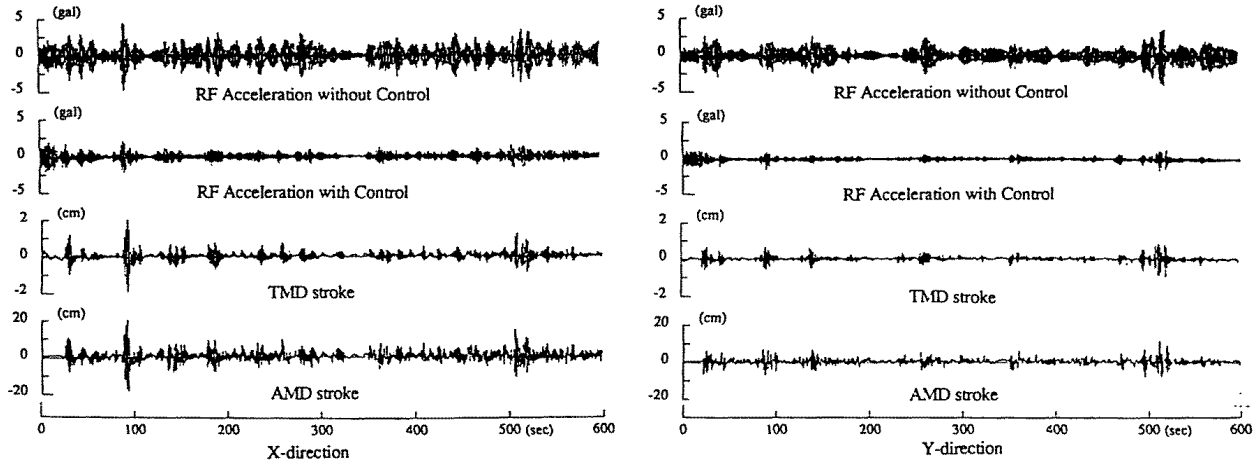

Figure 19. Observed/simulated responses (August 27 1993 typhoon).

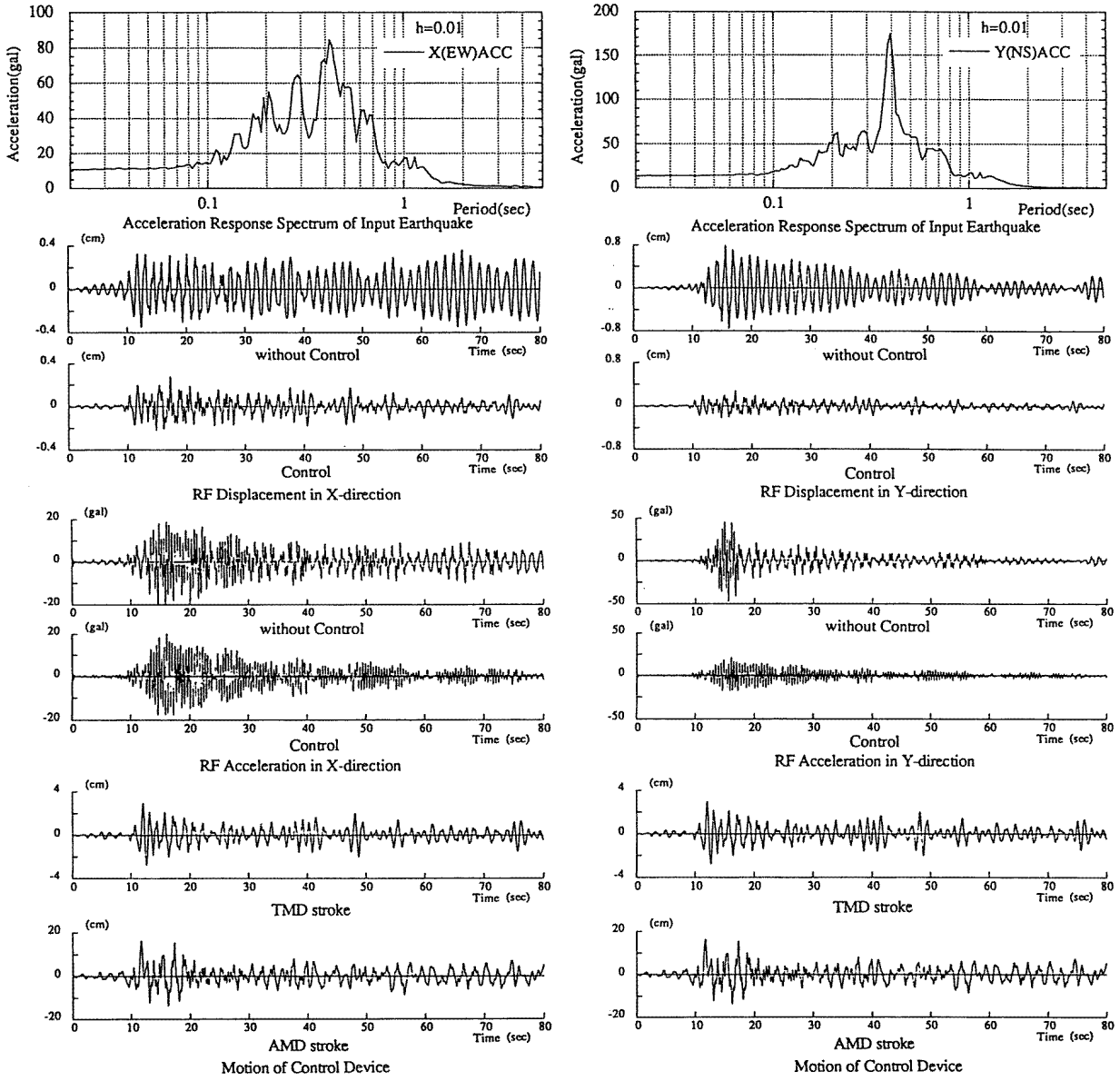

Figure 20. Observed/simulated responses (October 12 1993 earthquake).

The skeleton view of the composite TMD for this project is shown in figure 18. The whole moving mass, including TMD and AMD, is supported by four pieces of rubber bearings. Because of the material property, there is virtually no friction between the structure floor and the moving mass. The stiffness provided by the rubber material is uniform in all directions so that this device works as a pendulum with one modal period in universal directions. It is also noted that the whole system is covered with a housing so that the device can be exposed and placed on the roof floor.

It is also important to determine the target disturbance intensity. The purpose of the composite TMD is to improve the serviceability of the tall building under small earthquakes or relatively strong wind turbulences. Several earthquake records were used for the simulation that determined the linear control boundaries over which the feedback gains were naturally reduced so that the stable system could be designed.

Since this project was completed in 1992, we have had several opportunities to certify the performance of the device when it functioned during small earthquake events and windy weather occasions. The observed response vibration data, which were acquired during a typhoon that passed by in the vicinity in 1993, are shown in figure 19 where an analytical simulation without the composite TMD is also shown for comparison. The vibration control performance is well certified by observation and the post-analysis. When a relatively small earthquake happened on October 12 in 1993, we also obtained data which are shown in figure 20. In the case of the earthquake, the observed responses of the building's roof location were accurately simulated by only using the acceleration record at the basement floor. Hence, the identified mathematical model of the frame structure and the device dynamics were certified to be accurate enough to certify the controller's performance.

4. Closing remarks

The acceleration feedback method applied to the active TMD was discussed in this paper. The optimum parameters, minimization of control force, power and energy under various types of disturbance are methodologically obtained. Then, the algorithm is extended into a realistic multi-degree-of-freedom model to discuss stability criteria, tuning adjustment and the multi-modal control algorithm. A state estimator design is also proposed to that an additionally required two sensors are eliminated and tuning adjustment is made possible electrically instead of by mechanical stiffness adjustment. An application project is also introduced to show the feasibility of the algorithm strategy, which is verified by comparing the observed control performance and the analytical simulation.

References

[1] Brock J E 1946 A note on the damped vibration absorber *Trans. ASME, J. Appl. Mech.* **13** A-284

[2] Chang J and Soong T T 1980 Structural control using active tuned mass dampers *J. Eng. Mech. Div. ASCE* **106** 1081–8

[3] Crandall S H and Mark W D 1963 *Random Vibration in Mechanical Systems* (New York: Academic)

[4] Den Hartog J P 1957 *Mechanical Vibrations* 4th edn (New York: McGraw-Hill)

[5] Frahm U 1909 *US Patent* 989 958

[6] Hahnkamm E 1932 *Ann. Phys. Lpz.* **14** 683

[7] Hahnkamm E 1935 *Versammlung der Schiffbautechnische Gesellschaft* (Berlin)

[8] Kobori T *et al* 1991 Seismic response controlled structure with active mass driver system, part 1 and part 2 *Earthquake Eng. Struct. Dyn.* **20** 133–49

[9] Koshika N *et al* 1993 Research, development and application of active–passive composite tuned mass damper *4th Int. Conf. on Adaptive Structures (Cologne, 1993)*

[10] Lund R A 1979 Active damping of large structures in winds *ASCE Convention (Boston, MA, 1979)*

[11] Morison J and Karnopp D 1973 Comparison of optimized active and passive vibration absorber *14th Annu. Joint Automatic Control Conf. (OH)* pp 932–8

[12] McNamara R J 1977 Tuned mass dampers for buildings *Trans. ASCE J. Struct. Div.* **103** 1785–98

[13] Nishimura I *et al* 1992 Active tuned mass damper *Smart Mater. Struct.* **1** 306–11

[14] Nishimura I *et al* 1992 Active passive composite tuned mass damper *Proc. ATC17-1 (San Francisco)* pp 737–43

[15] Nishimura I *et al* 1994 The optimal active tuned mass damper under random excitation *Proc. 5th Int. Conf. on Adaptive Structures (Sendai, 1994)*

[16] Nishimura I 1994 Vibration control of building structures by active tuned mass damper *Doctoral Dissertation* Graduate School of Engineering, University of Tokyo submitted

[17] Nishimura I *et al* 1994 Acceleration feedback method applied to active–passive composite tuned mass damper *J. Struct. Control.* **1** 103–16

[18] Ormondroyd J and Den Hartog J P 1928 The theory of the dynamic vibration absorber *Trans. ASME* **50**

[19] Petersen N R 1979 Design of large-scale tuned mass damper *ASCE Natl. Convention (Boston, MA, 1979)*

[20] Sakamoto M *et al* 1994 Practical applications of active and hybrid response control systems and their verifications by earthquake and strong wind observations *1st World Conf. on Structural Control (Los Angeles, CA, 1994)*

[21] Shiba K *et al* 1994 Vibration control characteristics of a hybrid mass damper system through earthquake observation records of a tall building *Proc. 1st World Conf. on Structural Control (Los Angeles, CA, 1994)* vol 1

[22] Soong T T 1988 State-of-the-art review: active structural control in civil engineering *J. Eng. Struct.* 74–84

[23] Tanida K *et al* 1993 Development of V-shaped hybrid mass damper and its application to high-rise buildings *Proc. Int. Workshop on Structural Control* pp 509–20

[24] Warburton G B 1982 Optimum absorber parameters for various combinations of response and excitation parameters *Earthquake Eng. Struct. Dyn.* **10** 381–401

[25] Yamada T, Kobori T and Nishimura I 1988 Dynamic vibration absorber *Japan Patent Bureau* S63-156171 submitted